ANTIMICROBIAL AGENTS AND CHEMOTHERAPY, Jan. 2006, p. 336–343 Vol. 50, No. 1
0066-4804/06/$08.00+0 doi:10.1128/AAC.50.1.336–343.2006

VraSR Two-Component Regulatory System and Its Role in Induction of *pbp2* and *vraSR* Expression by Cell Wall Antimicrobials in *Staphylococcus aureus*†

Shaohui Yin,[1] Robert S. Daum,[1,2,3] and Susan Boyle-Vavra[1]*

Department of Pediatrics,[1] Committee on Microbiology,[2] and Committee on Molecular Medicine,[3] The University of Chicago, Chicago, Illinois 60637

Received 15 June 2005/Returned for modification 8 August 2005/Accepted 18 October 2005

The VraS/VraR two-component system (VraSR) regulates transcriptional induction of penicillin-binding protein 2 (encoded by *pbp2*) by vancomycin in *Staphylococcus aureus*. We have now defined the *vraSR* operon and determined that its induction by β-lactams as well as by vancomycin is autoregulated. Induction of the *pbp2* and *vraSR* operons by β-lactams and related compounds within 1 hour after exposure to the antimicrobials was dependent on *vraS*. However, when a disk diffusion assay that can detect induction of genes over an extended time period was used, induction of the *pbp2* operon was mediated by some β-lactams, including oxacillin; this induction was independent of *vraS*.

In *Staphylococcus aureus*, penicillin-binding protein 2 (PBP 2) is one of four native penicillin-binding proteins (5, 12, 15, 16, 20). This essential protein plays an accessory role in methicillin and vancomycin (VAN) resistance (3, 4, 11, 14, 16–18). We previously demonstrated that *pbp2* transcription is inducible by the glycopeptide VAN and the β-lactam oxacillin (OXA) (a congener of methicillin) in all strains tested and that an undefined factor(s) induced by VAN binds to the *pbp2* promoter (3). A VAN- and β-lactam-inducible two-component regulatory system (VraSR) consisting of a sensor kinase (VraS) and response regulator (VraR) (9) was then found to control VAN-dependent induction of *pbp2* transcription as well as that of other cell wall biosynthesis genes (7). This regulatory system has also been found by other investigators to be induced by β-lactams and other cell wall agents in a variety of genetic backgrounds (13, 19). None of these previous studies have investigated whether induction of *pbp2* and *vraSR* by β-lactams is dependent on VraSR.

Since susceptibility to β-lactams decreased in a *vraSR* mutant (7), we investigated whether *vraSR* is also involved in β-lactam-induced transcription of *pbp2*. We accomplished this by constructing a *vraSR* mutant strain (M1) in the background of strain RN4220. Expression of *vraSR* and *pbp2* operons was studied in the wild type and in the *vraSR* mutant by Northern blot analysis and measurement of expression from *lacZ* fusions. The fragments for constructing *lacZ* fusions were cloned from the *pbp2* and *vraSR* operons from a previously characterized methicillin-resistant *S. aureus* (MRSA) isolate (strain IL-A) (2). All strains and plasmids used in this study are shown in Table 1. Table 2 shows the primer pairs used to amplify fragments for cloning. The primer sequences are available in Table S1 in the supplemental material.

* Corresponding author. Mailing address: Department of Pediatrics, The University of Chicago, 5841 S. Maryland Ave., MC 6054, Chicago, IL 60637. Phone: (773) 702-6401. Fax: (773) 702-1196. E-mail: sboyleva@midway.uchicago.edu.

† Supplemental material for this article may be found at http://aac.asm.org/.

To disrupt the *vraS* gene in the chromosome of strain RN4220, a *vraS* allelic replacement vector was constructed (pVRASR-erm-pCL52.1 [Table 1]). This consisted of a chimera between the *S. aureus* allelic replacement vector, pCL52.1 (10), and pVRASR-erm (Table 1). The latter is a plasmid constructed for this study that contains a *vraSR* insert (PCR amplified from strain IL-A) harboring an *ermC* cassette within the EcoRI site of *vraS*. pVRASR-erm-pCL52.1 was introduced into strain RN4220 by electroporation (1). The integration of the plasmid by homologous recombination and curing of the allelic replacement vector was accomplished by alternate rounds of incubation at the permissive (30°C) and nonpermissive (42°C) temperatures for replication of pCL52.1. An erythromycin (ERY)-resistant (Ery^r) and tetracycline-susceptible (Tet^s) colony that had been cured of the allelic replacement vector was chosen for further study. This mutant (M1) contained *ermC* inserted into the chromosomal *vraS* gene (Fig. 1A), as determined by use of PCR and Southern hybridization with *vraS* and *ermC* probes (not shown).

In the absence of antibiotics (uninduced condition), a low-abundance transcript (ca. 2.7 kb) was detected in strains RN4220 and M1 by Northern blotting (Fig. 1B) using a probe (depicted beneath the map in Fig. 1A) that spanned portions of both *vraS* and *vraR*. In the presence of low levels of VAN or OXA, an increase in the abundances of the 2.7-kb transcript and of several additional transcripts was detected in strain RN4220 (Fig. 1B). Similar results were observed for a clinical MRSA strain, IL-A (data not shown). In strain M1, induction of *vraSR*-specific transcripts by either VAN or OXA was drastically attenuated (Fig. 1B). These data support a model that induction of the *vraSR* operon by either VAN or OXA is autoregulated. The faint transcript in strain M1 also hybridized with an *ermC*-specific probe but not with a probe that was specific for *vraR* only (data not shown). These data suggest that the *vraS*-specific transcript in strain M1 consists of *orf1*, *yvqF*, a portion of *vraS*, and *ermC*. Thus, introduction of the *ermC* cassette into *vraS* likely introduced a negative polar effect on transcription of *vraR* downstream of the *ermC* insertion.

TABLE 1. Strains and plasmids

Strain or plasmid	Relevant features[a]	Reference or source
S. aureus strains		
RN4220	*S. aureus* intermediate host strain (restriction negative) for cloning (derived from strain 8325-4)	6
M1	*vraSR* mutant of RN4220 with *ermC* insertion in the EcoRI site of *vraS*, erythromycin resistant	This study
IL-A	MRSA clinical strain	2
Plasmids		
pGEM-T	*Escherichia coli* vector, ampicillin resistance (*blaZ*)	Promega
pAW8	*S. aureus-E. coli* shuttle vector, Tet^r, intergenic region from pUC118, pAMα1 gram-positive ori and ColE1 ori from *E. coli*	Akihito Wada
pCMVβ	Vector used as a source for *lacZ* gene	Clontech
pALC80	Used as a source for *ermC* gene; pSPT181 containing a 2.4-kb *sar* fragment carrying *ermC* gene, stable at 32°C	Ambrose Cheung
pCL52.1	*E. coli-S. aureus* shuttle plasmid; gram-positive Ts ori from pE194; Spx^r; Tet^r gene from pT181	Chia Lee (10)
pVRASR-1	pGEM-T containing cloned *vraSR* PCR fragment	This study
pVRSASR-erm	pVRASR-1 containing *ermC* in the EcoRI site of *vraS*	This study
pVRASR-erm-pCL52.1	PstI-digested pVRASR-erm ligated with PstI-digested pCL52.1	This study
pVP1	pAW8 containing a translational fusion between the *vraSR* operon fragment, VP1, from strain IL-A and *lacZ* from pCMVβ	This study
pVP1′	pAW8 containing a translational fusion between the *vraSR* operon fragment, VP1′, from strain IL-A and *lacZ* from pCMVβ	This study
pVP2	pAW8 containing a *lacZ* translational fusion between the *vraSR* operon fragment, VP2, from MRSA strain IL-A and *lacZ* from pCMVβ	This study
pVP2′	pAW8 containing translational fusion between *vraSR* operon fragment, VP2′, from MRSA strain IL-A and *lacZ* from pCMVβ	This study
pVP-262	pAW8 containing a translational fusion between the VP-262 fragment from the *vraSR* operon from MRSA strain IL-A and *lacZ* from pCMVβ	This study
pVP-462	pAW8 containing a translational fusion between the VP-462 fragment from the *vraSR* operon from MRSA strain IL-A and *lacZ* from pCMVβ	This study
pPBP2-b	pAW8 containing a translational fusion between the *pbp2* operon fragment, PBP2-b, from MRSA strain IL-A and *lacZ* from pCMVβ	This study
pPBP2-c	pAW8 containing a translational fusion between the *pbp2* operon fragment, PBP2-c, from MRSA strain IL-A and *lacZ* from pCMVβ	This study

[a] The *lacZ* fragment in all *lacZ* fusions begins at the 33rd codon; ori, origin of replication; Ts, temperature sensitive.

A previous report speculated that the *vraSR* operon was comprised solely of *vraS* and *vraR* (7). Since the longest *vraSR*-specific transcripts (2.7 and 3 kb in size) we detected are larger than the combined size of the *vraS* and *vraR* open reading frames (ORFs) (1.7 kb), we investigated whether two additional ORFs (*orf1* and *yvqF*) located immediately upstream of *vraS* (Fig. 1A) (8) are cotranscribed with *vraS* and *vraR*. This was accomplished with primers PE1 to PE3 (Fig. 1A) by use of assay conditions described previously (16). A major transcription start point (tsp) was detected

TABLE 2. Primer pairs used for producing PCR fragments

Fragment	Primer		Size (bp)	Resulting plasmid
	Forward	Reverse		
lacZ fragment for creating fusions	lacF2-BamHI	lacR1-PstI		pVRASRerm-pCL52.1
vraSR operon fragments	vraSR-F	vraSR-R	1,700	pVRASRerm
vraSR probe	vraSRprobeF	vraSRprobeR	2,022	None (not cloned)
VP1	VraF1-KpnI	VraR1-BamHI	1,183	pVP1
VP1′	VraF2-KpnI	VraR1-BamHI	1,513	pVP1′
VP2	VraF3-KpnI	VraR2-BamHI	1,076	pVP2
VP2′	VraF4-KpnI	VraR2-BamHI	2,218	pVP2′
VP-262	VraF5-KpnI	VraR3-BamHI	412	pVP-262
VP-462	VraF6-KpnI	VraR3-BamHI	612	pVP-462
pbp2 operon fragments				
PBP2-a	PBP2F1-KpnI	PBP2R1-PstI	326	pPBP2-a
PBP2-b	PBP2F1-KpnI	PBP2R2-PstI	955	pPBP2-b
PBP2-c	PBP2F2-KpnI	PBP2R2-PstI	647	pPBP2-c
PBP2-d	PBP2F3-KpnI	PBP2R2-PstI	431	pPBP2-d

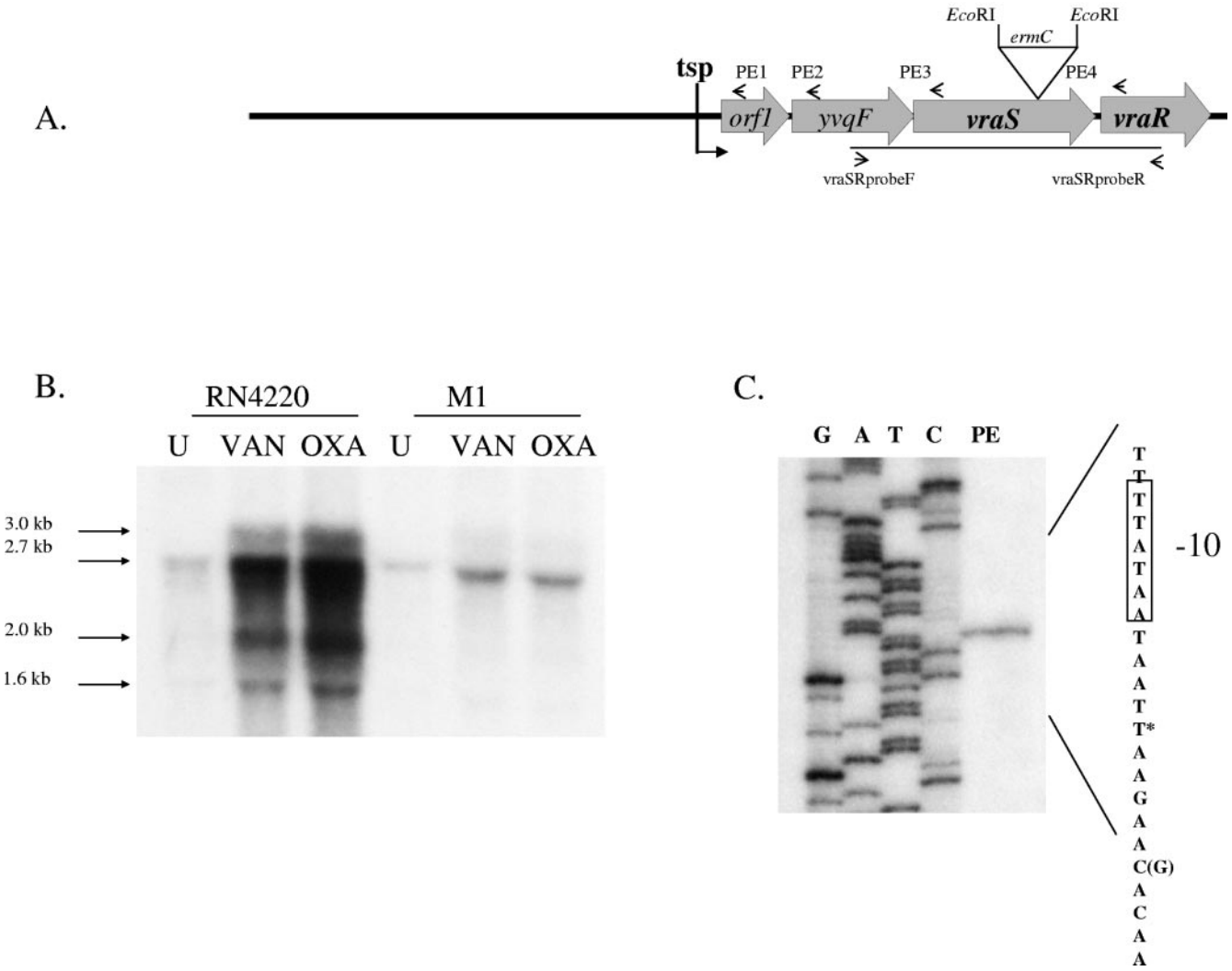

FIG. 1. Northern blotting analysis of *vraS* transcripts in wild-type strain RN4220 and the *vraS* mutant strain (M1) treated with VAN or OXA. (A) Map of the four ORFs contained in the *vraSR* operon illustrating the probe (line beneath map) used in Northern blotting analysis and the binding sites for primers (short arrows) (PE1 to PE4) used in the primer extension assay. The *vraSR* probe was PCR amplified using the primers vraSRprobeF and vraSRprobeR. The *vraSR* mutant (M1) contains an *ermC* cassette inserted into the EcoRI site of the chromosomal *vraS* gene, as depicted above the map. (B) Northern blot of RNA isolated from uninduced cultures (U) or cultures induced by VAN (2 μg/ml) or OXA (1 μg/ml). Membranes were hybridized with a *vraSR*-specific probe (shown beneath the map in panel A). Overnight cultures of *S. aureus* strains were diluted 1:100 in tryptic soy broth (10 ml in a 50-ml conical Falcon tube), shaken at 250 rpm, and grown at 37°C. After a 1-h incubation, the cultures were treated and incubated for another hour. The *vraSR* probe was PCR labeled with [α-^{32}P]dATP (Amersham) using the Prime-a-Gene labeling system (Promega). The hybridized blots were washed with 0.1× SSC buffer (1× SSC is 0.15 M NaCl plus 0.015 M sodium citrate) containing 0.1% sodium dodecyl sulfate four times at 70°C, each time for 30 min. (C) Results from primer extension (PE) analysis of MRSA strain IL-A with the use of primers PE1, PE2, and PE3. The asterisk indicates the major tsp. The reaction product was mixed with half the volume of a sequencing stop solution, denatured, and applied to a 5% sequencing gel. The sequencing ladder (lanes labeled G, A, T, C) was prepared by using an *fmol* DNA cycle sequencing system (Promega) with the same primer used in the primer extension reaction.

132 bp upstream of the *orf1* translation start codon in strains M1, RN4220, and IL-A (Fig. 1C). A minor tsp (a faint product) was also found 48 bp upstream of the *orf1* translation start codon (data not shown). No product was detected using primer PE4. Thus, the *vraSR* operon consists of four ORFs with a major tsp (Fig. 1A).

To confirm the conclusions from the primer extension analysis, several *vraSR-lacZ* fusions were constructed (Table 1). Since an *S. aureus* ribosome binding site optimizes expression of foreign proteins, *lacZ* translational fusions were constructed. Fragments encompassing various regions of the *vraSR* operon, as shown in Fig. 2A, were PCR amplified from strain IL-A (primer pairs listed in Table 2). To facilitate cloning, the forward and reverse primers contained terminal KpnI and BamHI recognition sequences, respectively. Two *vraSR* operon fragments ended with the sixth codon of *orf1* (VP-462 and VP-262), two fragments ended with the sixth codon of *vraS* (VP1′ and VP1), and two fragments ended with the sixth codon of *vraR* (VP2′ and VP2). A 3,051-bp *lacZ* gene fragment starting with the 33rd codon was obtained by PCR amplification from pCMVβ by use of forward and reverse primers (listed in Table 2) containing BamHI and KpnI recognition

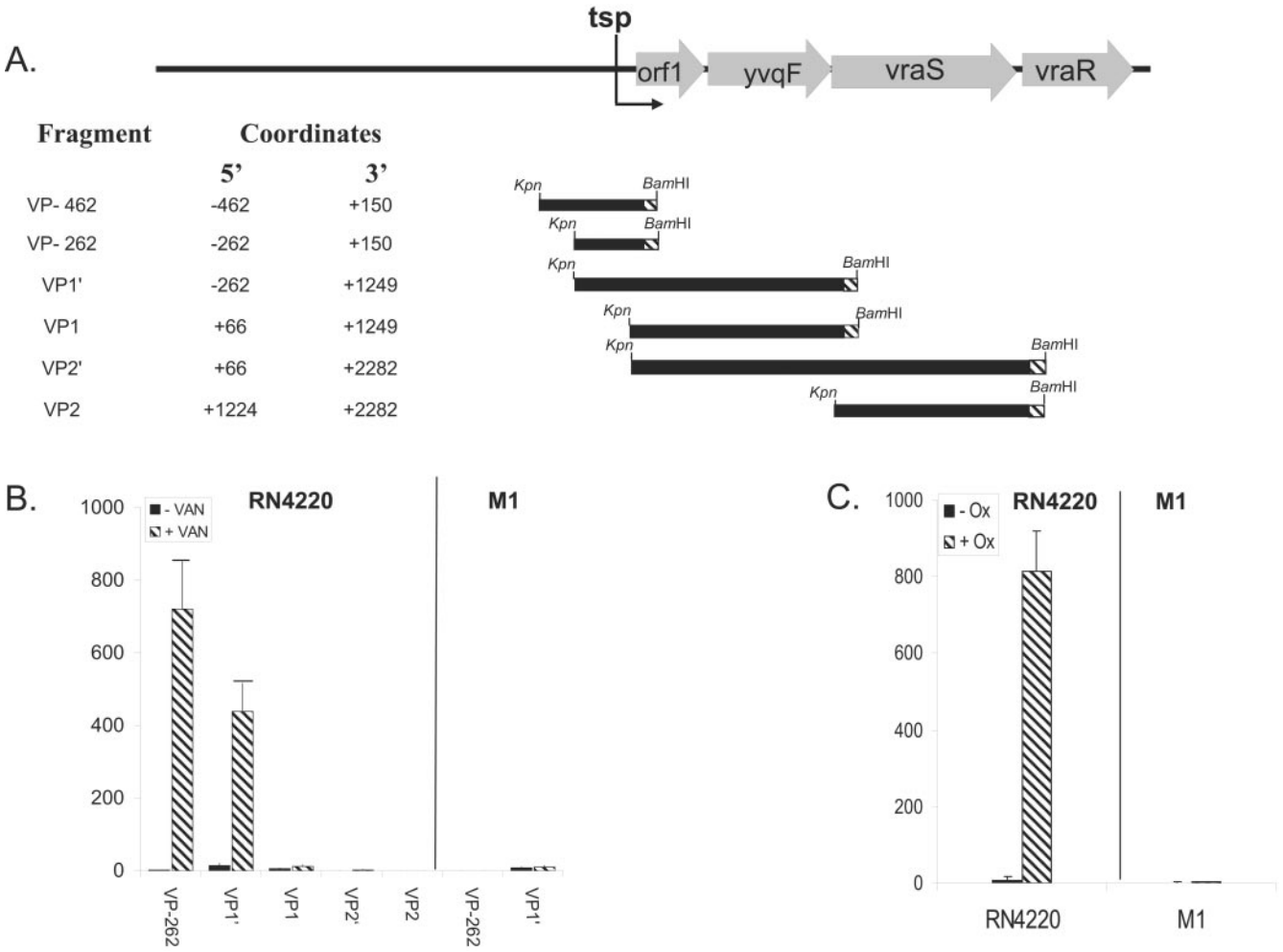

FIG. 2. Analysis of *vraSR-lacZ* fusions by β-galactosidase assay in wild-type strain RN4220 and the *vraSR* mutant (M1). (A) Map of the DNA fragments (horizontal black bars beneath the map) PCR amplified from the *vraSR* operon from MRSA strain IL-A, which was used to produce the *vraSR-lacZ* fusions. PCR primers were designed with KpnI (forward primers) and BamHI (reverse primers) restriction enzyme recognition sequences to facilitate cloning of the fragments. Fragment coordinates are relative to the *vraSR* tsp determined as shown in Fig. 1C. Each square filled with diagonal lines at the end of each fragment represents the amino terminus of the corresponding ORF to which *lacZ* was joined. VP-462 and VP-262 terminate with the sixth codon of *orf1*, VP1 and VP1′ terminate with the sixth codon of *vraS*, and VP2′ and VP2 terminate with the sixth codon of *vraR*. To optimize translation of *lacZ* in *S. aureus*, each fragment was fused upstream of, and in frame with, the 33rd codon of a 3,051-bp *lacZ* fragment isolated by PCR from pCMVβ (primer pairs in Table 2). Each PCR fragment was digested with KpnI and BamHI and ligated upstream of the *lacZ* fragment (Table 2) in pAW8 (18). (B) β-Galactosidase assays of VAN-specific induction of *vraSR-lacZ* fusions in wild-type strain RN4220 and *vraSR* mutant strain M1. The data are the means of at least three experiments. Error bars represent the standard deviations of the means. (C) β-Galactosidase assays of OXA (Ox)-specific induction of *vraSR-lacZ* constructs harbored in RN4220 or strain M1. β-Galactosidase specific activity was expressed as nanomoles of product formed per minute per mg of protein at 37°C.

sequences, respectively. Each *vraSR* fragment was cloned upstream of and in frame with the *lacZ* fragment in the KpnI site of pAW8, a gram-positive shuttle plasmid. The resulting *lacZ* fusion plasmids were given names that reflect the fragments that were placed upstream of *lacZ*; accordingly, pVP-262 contains fragment VP-262, etc. (Table 1). Strains RN4220 and M1, harboring plasmid pVP-262, pVP1′, pVP1, pVP2′, or pVP2, were incubated at 37°C in the presence of VAN (1 μg/ml) for 1 hour, conditions previously determined to demonstrate induction of *pbp2* (3). β-Galactosidase activity was measured (Stratagene kit) using extracts prepared by lysostaphin (Sigma)-aided cell lysis (3). β-Galactosidase specific activity was expressed as nanomoles of product formed per minute per mg of lysate at 37°C.

Of the plasmids tested in strain RN4220, only pVP-262 and pVP1′, which harbored inserts spanning the tsps identified above, were significantly induced by VAN (Fig. 2B) ($P < 0.001$; two-tailed Student's *t* test). VAN-dependent induction of β-galactosidase activity from pVP-262 was ablated in strain M1 (Fig. 2B), a finding consistent with the Northern blotting results (Fig. 1B). The amount of β-galactosidase activity produced from strain RN4220 in the presence of VAN decreased precipitously for pVP1 compared with results for pVP1′ (Fig. 2B). These data indicate that a region which encompasses the

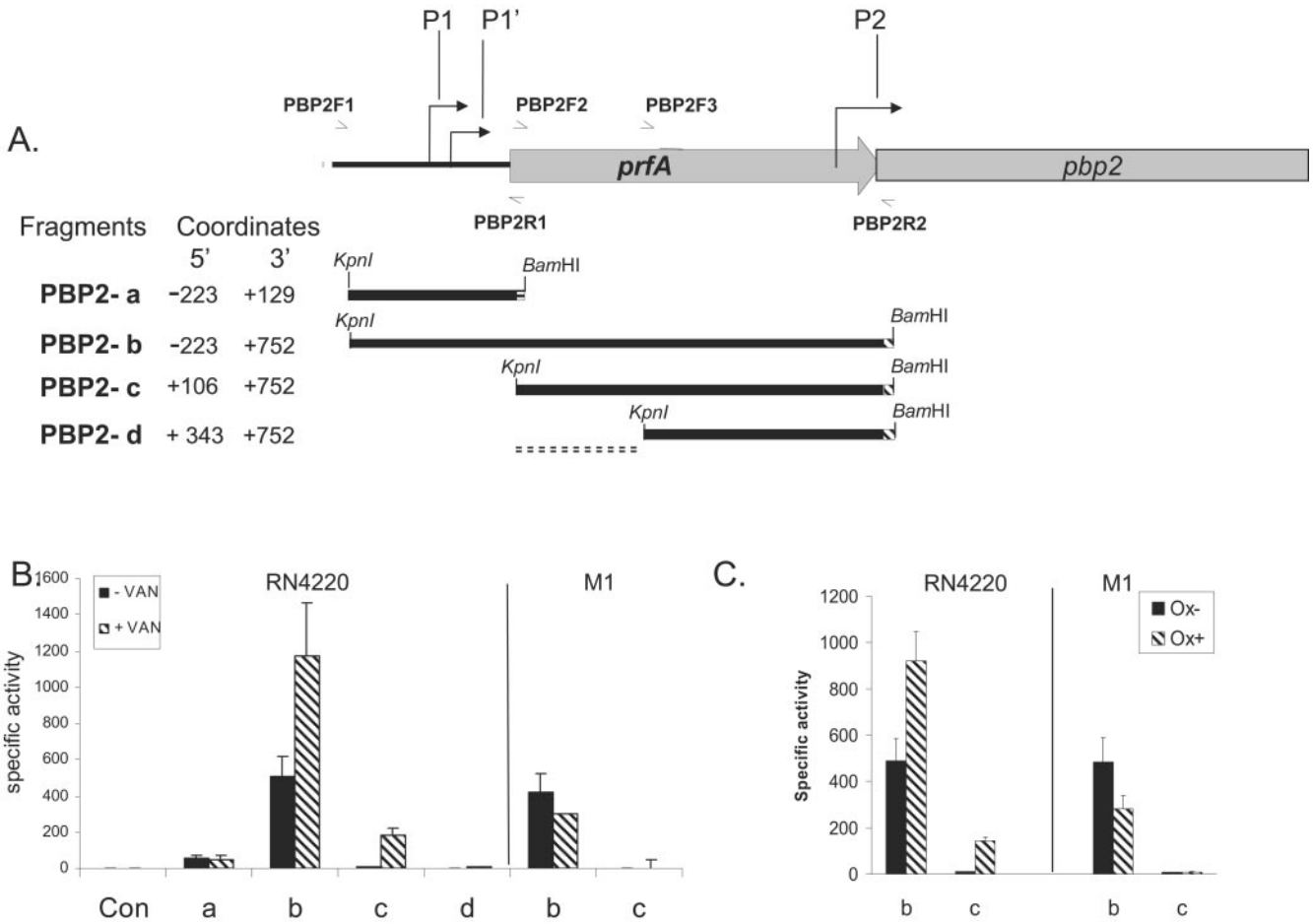

FIG. 3. Analysis of *pbp2-lacZ* fusions by β-galactosidase assay in wild-type strain RN4220 and the *vraSR* mutant (M1). (A) Map of the *pbp2* operon and PCR fragments (horizontal bars beneath map) encompassing its various regions that were fused upstream of and in frame with *lacZ*. The three tsp's (P1, P1′, and P2) and various primers used in this study (half arrowheads) are shown relative to the *prf* and *pbp2* ORFs. Coordinates are relative to the P1 tsp, with accession number AB035448 used as a reference sequence. The operon fragments in pPBP2-b, pPBP2-c, and pPBP2-d each terminate after the eighth codon of *pbp2* (square filled with diagonal lines). The fragment in pPBP2-a terminates after the sixth codon of *prfA* (square filled with horizontal lines). (B) VAN-specific induction *pbp2-lacZ* fusions pPBP2-a (a), pPBP2-b (b), pPBP2-c (c), and pPBP2-d (d) in wild-type strain RN4220 and in M1. Con, RN4220 harboring vector containing only the *lacZ* insert. The data represent the means of at least three experiments. Error bars represent the standard deviations of the means. (C) OXA (Ox)-dependent induction of *pbp2-lacZ* fusions pPBP2-b (b) and pPBP2-c (c) in strains RN4220 and M1. β-Galactosidase specific activity was expressed as nanomoles of product formed per minute per mg of protein at 37°C.

tsp's (from −262 to +65 relative to the major tsp) was important for high-level VAN-dependent induction of the *vraSR* operon in the wild-type strain. The small amount of both induced and uninduced β-galactosidase activity from fragments VP1, VP2′, and VP2 is consistent with the absence of detection of primer extension products (Fig. 1) from the corresponding portions of the operon.

As seen for VAN, OXA also significantly induced (107-fold; $P < 0.001$) β-galactosidase activity produced from the *vraSR* operon, as seen in strain RN4220 harboring pVP-462 (Fig. 2C). OXA-dependent induction of pVP-462 was VraSR dependent, since it was ablated in strain M1. These data along with the Northern blotting data (Fig. 1B) support the conclusion that both VAN- and OXA-dependent inductions of the VraSR operon are autoregulated. The sequence of the promoter region in strain M1 was the same as that in RN4220 (including 843 bp upstream and 163 bp downstream of the major tsp), a finding that ruled out the possibility that the observed down-modulation of *vraSR* in strain M1 could be due to a spontaneous *cis*-acting mutation.

The *pbp2* operon consists of two ORFs (*prfA* and *pbp2*) (16). Three separate transcripts (3) have been previously detected from three identified transcription start sites (P1, P1′, and P2) (Fig. 3) (16). To delineate the *cis*-acting sequences in the *pbp2* operon responsive to *vraSR*-regulated transcriptional induction by VAN and OXA, four fragments (PBP2-a through PBP2-d) were isolated by PCR from MRSA strain IL-A (Fig. 3A and Table 2) and inserted in pAW8 upstream of, and in frame with, a *lacZ* fragment that starts with the 33rd codon. The resulting plasmids (pPBP2-a, pPBP2-b, pPBP2-c, and pPBP2-d) (shown in Fig. 3 and Table 1) contained either a *prfA-lacZ* translational fusion (pPBP2-a) or *pbp2-lacZ* translational fusions with progressive 5′ deletions (pPBP2-b, -c, and -d), as depicted in Fig. 3A.

The ability of VAN (Fig. 3B) or OXA (Fig. 3C) to induce expression from each construct was tested in the wild-type strain, RN4220, and the *vraSR* mutant, M1. β-Galactosidase activity from strain RN4220 containing a negative control (pAW8 containing the *lacZ* fragment) was negligible in either the presence or the absence of antibiotics (Fig. 3A). Even when the plasmids were harbored in RN4220, the β-galactosidase activities of pPBP2-a and pPBP2-d were low, and no induction by VAN was observed (Fig. 3B). Such low induction of pPBP2-a was surprising, since it contains two (P1 and P1′) of the three tsp's in this operon. This result could be explained by the absence of the third tsp (P2) (Fig. 3A). However, since expression of β-galactosidase activity from pPBP2-a is driven by a translational fusion, the low-induction phenotype may also be explained by posttranscriptional influences on *prfA* expression.

When expressed in strain RN4220, pPBP2-b (which contained all three tsp's) produced significantly more β-galactosidase activity than any of the other constructs tested from this operon ($P < 0.001$) in either the presence or the absence of an inducing antimicrobial. The β-galactosidase activity decreased significantly ($P < 0.001$) with each progressive 5′ deletion in the *pbp2* operon (pPBP2-b, -c, and -d) (Fig. 3B). The β-galactosidase activity expressed from pPBP2-b significantly increased ($P \leq 0.001$) in the presence of either VAN (Fig. 3B) or OXA (Fig. 3C) in strain RN4220. Although the amount of β-galactosidase activity produced by strain RN4220 harboring pPBP2-c under any condition was small compared with that produced by RN4220 harboring pPBP2-b, expression from the former construct was nevertheless induced 16- and 13-fold by VAN and OXA, respectively, relative to the untreated control. The β-galactosidase activity induced by either VAN or OXA from pPBP2-b and pPBP2-c was ablated in strain M1 (Fig. 3B). Thus, OXA-dependent as well as VAN-dependent induction of these fragments was dependent on VraSR. Since pPBP2-c and pPBP2-d both contained fragments with the same tsp (P2) and had common 3′ ends (Fig. 3A), their different induction profiles suggest that the 237-bp region in the N terminus of pPBP2-c (Fig. 1A) contains at least a portion of a VraSR-responsive sequence. This idea might also explain the low level of induction from pPBP2-a, which is also missing that region.

Uninduced β-galactosidase activity from pPBP2-b was not significantly lower in strain M1 than in RN4220 ($P = 0.1$) (Fig. 3B and C), a finding consistent with Northern blotting results for the chromosomal *pbp2* gene (data not shown). Uninduced expression levels of *vraSR* were also similar for strains RN4220 and M1 (Fig. 2). These data support the conclusion that while VraSR is required for OXA- and VAN-dependent induction of *pbp2* and *vraSR*, it is not required for uninduced expression of these operons.

Induction of two *lacZ* fusion constructs produced from the *pbp2* operon (pPBP2-b and pPBP2-c) and of one from the VraSR operon (pVP-262) was also tested by use of a disk diffusion assay. In this assay, antibiotic disks are placed over bacteria that are inoculated onto tryptic soy agar medium containing 5-bromo-4-chloro-3-indolyl-β-D-galactoside (X-Gal; 120 μg/ml). Induction of the *lacZ* reporter gene by the antibiotics was visualized as a blue rim at the edge of the zone of inhibition (Fig. 4). We used this assay to test the ability of a variety of cell wall antimicrobials, including VAN, OXA, cefotaxime (CTX), cefoxitin (FOX), cefaclor (CEC) and bacitracin (BAC), to induce *pbp2* and *vraSR* expression. The intensities of the blue color surrounding the zones of inhibition differed among the antibiotics (Fig. 4) for each of the three tested constructs (pPBP2-b, pPBP2-c, and pVP-462). The differences among antibiotics could be due to different agar diffusion rates of the various compounds or to differential activation of the *vraSR* operon. RN4220 harboring pAW8 containing the *lacZ* fragment (negative control) did not produce a blue rim (data not shown), providing evidence that induction was dependent on the inserted fragments.

In general, the antibiotic induction profiles produced by pPBP2-c and pVP-462 were very similar and differed from that of pPBP2-b, regardless of whether the construct was expressed in strain RN4220 or in the *vraS* mutant (Fig. 4). For example, in RN4220 containing pPBP2-c or pVP-462, β-galactosidase activity was visible only as a blue ring associated with cells growing at the rim around the zone of inhibition where the antibiotic could induce expression from the constructs. In contrast, strains that harbored pPBP2-b produced a similar ring but also produced blue product from bacteria growing over the entire plate (Fig. 4), a finding consistent with the high level of uninduced expression of that construct that we observed in the β-galactosidase assays (Fig. 3B).

In strain RN4220 harboring pPBP2-b, all the tested cell wall antimicrobials induced a distinct blue rim (albeit weakly for BAC), whereas only VAN, FOX, and CTX induced distinct blue rims from RN4220 harboring pPBP2-c or pVP-462. CEC did not induce detectable β-galactosidase activity from RN4220 harboring pPBP2-c or pVP-462, despite the distinct blue rims this same antibiotic induced in RN4220 harboring pPBP2-b (Fig. 4). OXA induced only a light blue rim from RN4220 harboring pVP-462 and no blue rim from RN4220 harboring pPBP2-c, findings consistent with the low OXA-induced β-galactosidase activity detected for these constructs in liquid assays (Fig. 3C). Differences in antibiotic concentrations, diffusion rates, or zone sizes do not explain these differences among constructs, since the dark blue rim around the CEC and OXA disks overlaid on strain RN4220 harboring pPBP2-b provided evidence for efficient diffusion.

As expected, VAN, FOX, and CTX lost the ability to mediate induction of β-galactosidase activity from pPBP2-c and pVP-462 in *vraSR* mutant strain M1 (Fig. 4). Surprisingly, induction of pPBP2-b by VAN, FOX, CEC, and OXA was not abolished in strain M1, although CTX- and BAC-mediated induction of pPBP2-b was abolished in that strain. Therefore, in this assay, the VraSR two-component regulatory system was not required for induction of pPBP2-b by VAN, FOX, CEC, or OXA, although VraSR was required for CTX-mediated induction of this construct. These data were surprising, since induction of pPBP2-b in broth culture after 1 hour of OXA or VAN induction was inhibited in strain M1 (Fig. 2).

That the induction profiles were more similar between the *pbp2-lacZ* fusion in pPBP2-c and the *vraSR-lacZ* fusion in pVP-462 suggests that the operon fragments in these constructs contain a *cis* element that responds to VraR or a VraR-regulated factor. Differences in expression between the two *pbp2* fragments cannot be explained by differences in post-translational regulation, since they both include the ribosome binding site and the first eight codons of the *pbp2* gene.

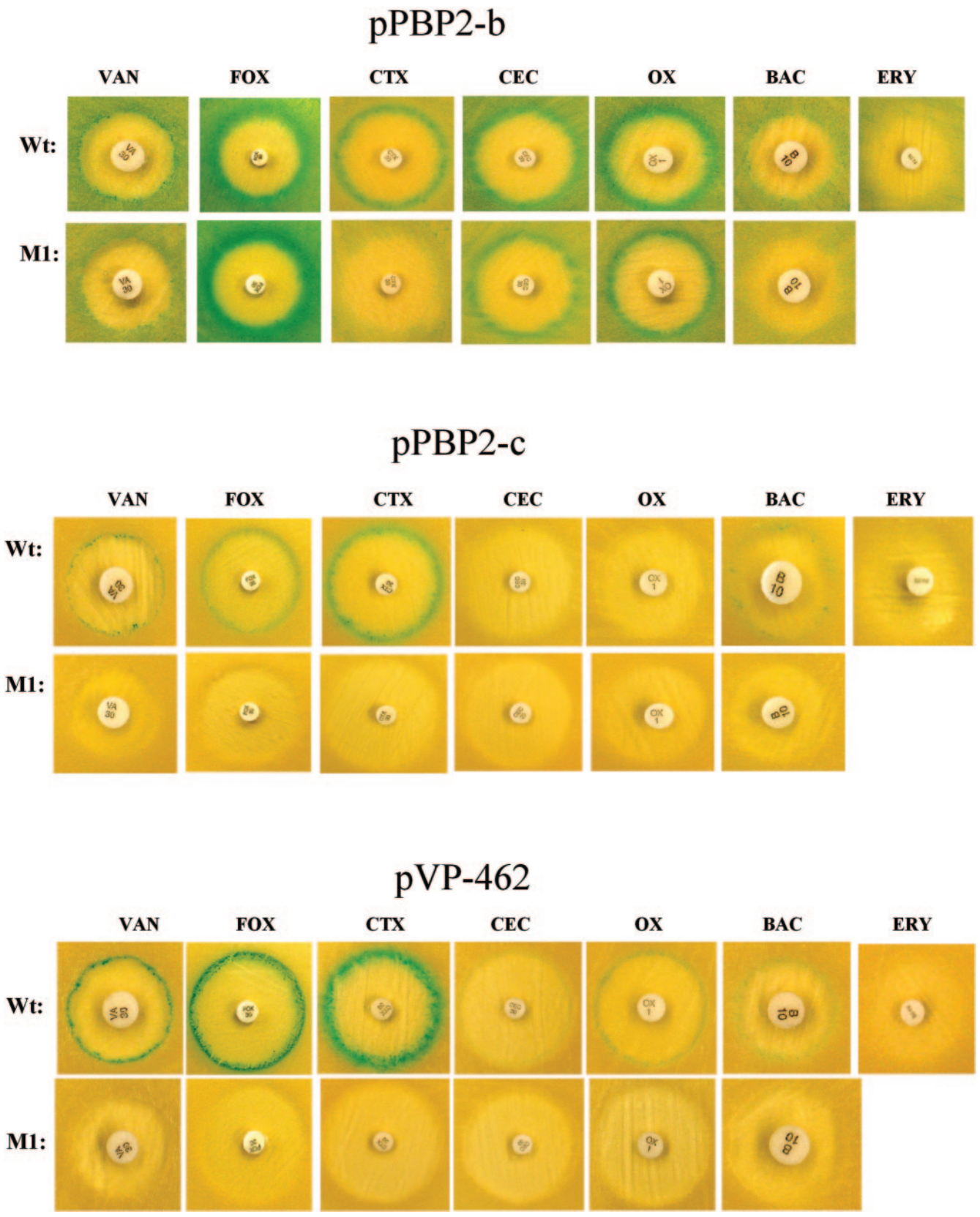

FIG. 4. Disk diffusion assay for induction of *pbp2*- and *vraSR-lacZ* fusions. Strain RN4220 (Wt) and the *vraSR* mutant strain (M1) carrying *pbp2-lacZ* fusions (pPBP2-b, pPBP2-c) or a *vraSR-lacZ* fusion (pVP-462) were diluted to the optical density of a 0.5 McFarland turbidity standard (BBL), swabbed onto tryptic soy agar containing TET (10 μg/ml) and X-Gal, overlaid with antibiotic-containing disks (Sensi-Disc; BBL), and incubated at 37°C overnight. Subsequent incubation at 4°C for 2 days intensified the blue color. The concentrations of the antibiotics were as follows: VAN, 30 μg; CTX, 30 μg; CEC, 30 μg; OXA (OX), 1 μg; FOX, 30 μg; BAC, 10 μg; ERY, 2 μg.

These data suggest that although short-term VAN- and OXA-mediated induction of *pbp2* and *vraSR* expression is VraSR dependent, longer-term induction of *pbp2* (i.e., pPBP2-b) is possible via a VraSR-independent pathway. However, long-term induction of pPBP2-b by CTX is dependent on VraSR.

The protein synthesis inhibitors ERY and clindamycin (data not shown) did not induce a blue rim from either RN4220 or M1 harboring either construct (data shown for pPBP2-b [Fig. 4]). Kuroda et al. reported that levofloxacin (7), a fluoroquinolone, did not induce *vraSR* transcription. Thus, only cell wall synthesis inhibitors have been shown to induce *vraSR* or *pbp2* transcription. This suggests that the induction of the *vraSR* regulon by cell wall antimicrobials is not due to a general stress response associated with growth inhibition by the antimicrobials.

Several reports have documented the genome-wide transcriptional response to cell wall antimicrobials in *S. aureus* by use of a microarray approach (7, 13, 19). Kuroda and colleagues (7) identified several cell wall biosynthesis genes that were induced by vancomycin in a *vraSR*-dependent fashion. These included the *pbp2* operon, *sgtB*, and *murZ*. These same genes were also reported by Pechous et al. (13) and Utaida et al. (19) to be induced by a variety of cell wall antibiotics, although the role of VraSR was not investigated. Our results have extended those studies by demonstrating that β-lactam-induced *pbp2* transcription is *vraSR* dependent, although some agents in this class appear to be less effective inducers than others. Additionally, we have demonstrated that β-lactam- and VAN-induced *vraSR* expression is autoregulated. Finally, we have shown that after long-term exposure to certain β-lactams, *S. aureus* is able to activate *pbp2* transcription via an alternate pathway in the absence of VraSR. These data provide a complex picture of VraSR activation that suggests a model involving both inhibition of cell wall synthesis and antibiotic interaction with the two-component regulatory system. The mechanism by which VraS senses diverse cell wall antimicrobial classes and how VraR interacts with the target promoter sequences are currently under investigation in order to better understand the mechanism of action of various cell wall agents.

This work was supported by NIH R01 AI40481-01A1 (to R.S.D. and S.B.-V.) and R03 AI44999-01 (to S.B.-V.). Shaohui Yin was supported by a grant from the Children's Research Foundation, Northbrook, IL.

REFERENCES

1. **Augustin, J., and F. Gotz.** 1990. Transformation of Staphylococcus epidermidis and other staphylococcal species with plasmid DNA by electroporation. FEMS Microbiol. Lett. **66:**203–208.
2. **Boyle-Vavra, S., R. B. Carey, and R. S. Daum.** 2001. Development of vancomycin and lysostaphin resistance in a methicillin-resistant Staphylococcus aureus isolate. J. Antimicrob. Chemother. **48:**617–625.
3. **Boyle-Vavra, S., S. Yin, M. Challapalli, and R. S. Daum.** 2002. Transcriptional induction of the penicillin-binding protein 2 gene in *Staphylococcus aureus* by cell wall-active antibiotics oxacillin and vancomycin. Antimicrob. Agents Chemother. **2003:**1028–1036.
4. **Hanaki, H., K. Kuwahara-Arai, S. Boyle-Vavra, R. S. Daum, H. Labischinski, and K. Hiramatsu.** 1998. Activated cell-wall synthesis is associated with vancomycin resistance in methicillin-resistant Staphylococcus aureus clinical strains Mu3 and Mu50. J. Antimicrob. Chemother. **42:**199–209.
5. **Henze, U. U., and B. Berger-Bachi.** 1995. *Staphylococcus aureus* penicillin-binding protein 4 and intrinsic β-lactam resistance. Antimicrob. Agents Chemother. **39:**2415–2422.
6. **Kreiswirth, B. N., S. Lofdahl, M. J. Betley, M. O'Reilly, P. M. Schlievert, M. S. Bergdoll, and R. P. Novick.** 1983. The toxic shock syndrome exotoxin structural gene is not detectably transmitted by a prophage. Nature **305:**709–712.
7. **Kuroda, M., H. Kuroda, T. Oshima, F. Takeuchi, H. Mori, and K. Hiramatsu.** 2003. Two-component system VraSR positively modulates the regulation of cell-wall biosynthesis pathway in *Staphylococcus aureus*. Mol. Microbiol. **49:**807–821.
8. **Kuroda, M., K. Kuwahara-Arai, and K. Hiramatsu.** 2000. Identification of the up- and down-regulated genes in vancomycin-resistant Staphylococcus aureus strains Mu3 and Mu50 by cDNA differential hybridization method. Biochem. Biophys. Res. Commun. **269:**485–490.
9. **Kuroda, M., T. Ohta, I. Uchiyama, T. Baba, H. Yuzawa, I. Kobayashi, L. Cui, A. Oguchi, K.-I. Aoki, Y. Nagai, J.-Q. Lian, T. Ito, M. Kanamori, H. Matsumaru, A. Maruyama, H. Murakami, A. Hosoyama, Y. Mizutani-Ui, N. K. Takahashi, T. Sawano, R.-I. Inoue, C. Kaito, K. Sekimizu, H. Hirakawa, S. Kuhara, S. Goto, J. Yabuzaki, M. Kanehisa, A. Yamashita, K. Oshima, K. Furuya, C. Yoshino, T. Shiba, M. Hattori, N. Ogasawara, H. Hayashi, and K. Hiramatsu.** 2001. Whole genomic sequencing of methicillin-resistant Staphylococcus aureus. Lancet **357:**1225–1240.
10. **Lin, W. S., T. Cunneen, and C. Y. Lee.** 1994. Sequence analysis and molecular characterization of genes required for the biosynthesis of type 1 capsular polysaccharide in *Staphylococcus aureus*. J. Bacteriol. **176:**7005–7016.
11. **Moreira, B., S. Boyle-Vavra, B. L. M. de Jonge, and R. S. Daum.** 1997. Increased production of penicillin-binding protein 2, increased detection of other penicillin-binding proteins, and decreased coagulase activity associated with glycopeptide resistance in *Staphylococcus aureus*. Antimicrob. Agents Chemother. **41:**1788–1793.
12. **Murakami, K., T. Fujimura, and M. Doi.** 1994. Nucleotide sequence of the structural gene for the penicillin-binding protein 2 of Staphylococcus aureus and the presence of a homologous gene in other staphylococci. FEMS Microbiol. Lett. **117:**131–136.
13. **Pechous, R., N. Ledala, B. J. Wilkinson, and R. K. Jayaswal.** 2004. Regulation of the expression of cell wall stress stimulon member gene *msrA1* in methicillin-susceptible or -resistant *Staphylococcus aureus*. Antimicrob. Agents Chemother. **48:**3057–3063.
14. **Pinho, M. G., H. de Lencastre, and A. Tomasz.** 2001. An acquired and a native penicillin-binding protein cooperate in building the cell wall of drug-resistant staphylococci. Proc. Natl. Acad. Sci. USA **98:**10886–10891.
15. **Pinho, M. G., H. de Lencastre, and A. Tomasz.** 2000. Cloning, characterization, and inactivation of the gene *pbpC*, encoding penicillin-binding protein 3 of *Staphylococcus aureus*. J. Bacteriol. **182:**1074–1079.
16. **Pinho, M. G., H. de Lencastre, and A. Tomasz.** 1998. Transcriptional analysis of the *Staphylococcus aureus* penicillin binding protein 2 gene. J. Bacteriol. **180:**6077–6081.
17. **Severin, A., S. W. Wu, K. Tabei, and A. Tomasz.** 2004. Penicillin-binding protein 2 is essential for expression of high-level vancomycin resistance and cell wall synthesis in vancomycin-resistant *Staphylococcus aureus* carrying the enterococcal *vanA* gene complex. Antimicrob. Agents Chemother. **48:**4566–4573.
18. **Sieradzki, K., and A. Tomasz.** 1999. Gradual alterations in cell wall structure and metabolism in vancomycin-resistant mutants of *Staphylococcus aureus*. J. Bacteriol. **181:**7566–7570.
19. **Utaida, S., P. M. Dunman, D. Macapagal, E. Murphy, S. J. Projan, V. K. Singh, R. K. Jayaswal, and B. J. Wilkinson.** 2003. Genome-wide transcriptional profiling of the response of Staphylococcus aureus to cell-wall-active antibiotics reveals a cell-wall-stress stimulon. Microbiology **149:**2719–2732.
20. **Wada, A., and H. Watanabe.** 1998. Penicillin-binding protein 1 of *Staphylococcus aureus* is essential for growth. J. Bacteriol. **180:**2759–2765.